X-ray Absorption Spectroscopic Study of Chemically and Electrochemically Li Ion Extracted $Li_yCo_{0.85}Al_{0.15}O_2$ Compounds

Min Gyu Kim and Chul Hyun Yo*

Department of Chemistry, Yonsei University, Seoul 120-749, Korea

Received: March 3, 1999; In Final Form: June 2, 1999

The local structure refinements for chemically and electrochemically Li ion extracted $Li_yCo_{0.85}Al_{0.15}O_2$ compounds have been investigated by Co K-edge X-ray absorption spectroscopy. In the X-ray absorption near-edge structure (XANES), the 1s → 3d transition at ∼7709.9 eV and 1s → 4p transition at ∼7727.8 eV for the pristine $LiCo_{0.85}Al_{0.15}O_2$ have shifted effectively to higher energy regions of ∼0.6 eV and ∼2.5 eV for the higher Li ion extraction, respectively, which shows that the average oxidation state of Co ion increases gradually with the extraction. The systematic variations of peak intensities for the 1s → 3d transition and 1s → 4p transition result from Co 3d and 4p orbital mixing by the local structure distortion around Co atoms. In particular, the abrupt decrease of peak intensity for 1s → 4p transition with shakedown process by ligand to metal charge transfer (LMCT) represents the transfer of the hole state from the oxygen to Co atom and the localization at the Co atomic site as a form of Co^{IV} ion by structural distortion. The XANES features for the electrochemical extraction have shown that the electrochemical redox reaction is always not reversible in the Li ion extraction/insertion process. From the extended X-ray absorption fine structure (EXAFS) refinement, the interatomic distances of bond pairs decrease for the Li ion extraction. The chemical and electrochemical extractions have a significant effect on Fourier transform (FT) magnitude, which decreases linearly with the extraction. Since single and multiple scatterings with Co atoms have predominantly contributed to the FT magnitudes, the systematic decrease of FT magnitude is closely related to the static disorder of two different oxidative Co^{III} and Co^{IV} ions. This fact is consistent with the increase of the Debye−Waller factor for each bond pair.

Introduction

$LiMO_2$ (M = 3d transition metal elements) compounds have been extensively investigated as attractive cathodes for the rechargeable lithium battery.[1−6] In particular, much research on the electrochemical and physical properties of the $LiCoO_2$ has been carried out for applications of its high energy density and stability.[7−13] Recently, the partial substitutions of some special metals for the Co atom have been followed experimentally in order to obtain higher voltage cathode materials.[14−17] As the results, a high equilibrium potential (open-circuit voltage) has been obtained theoretically and experimentally for the Al substitution and increased systematically with Al content in $LiCo_{1-x}Al_xO_2$ oxides ($0 < x < 1$).[18] In this case, it has been suggested that the electrochemical property is correlated with the participation of the oxygen 2p band and the structural stability of Li ion extracted $Li_yCo_{1-x}Al_xO_2$ compounds ($0 < y < 1$). Since very high Li ion extraction gives rise to the bulk structural destabilization by electrostatic repulsion within the lattice, the layer structure cannot be maintained above a critical *y* value. Therefore, it is very important to determine the relationship between the local structure and the degree of Li ion extraction.

The Li ion chemical extractions for the $LiMO_2$ have been also tried in various aqueous environments in order to establish the structural variation and the extraction mechanism.[19−22] Using many acids and oxidizing agents, the variations of bulk structure and chemical composition have been found with XRD and chemical analysis, respectively.[23] However, the line broadening of the X-ray diffraction peak due to chemical treatment makes it difficult to determine the precise lattice structure. Furthermore, the local structure refinements around Co atoms are impossible to carry out critically with only XRD patterns since XRD methodology is limited to bulk structural property. The general variation of lattice parameters has only been identified in the viewpoint of bulk structure.

Recently, a new structural analysis of X-ray absorption (XANES/EXAFS) spectroscopy has been used for a local structure refinement on an interesting atom. The absorption peak features in the X-ray absorption near-edge structure (XANES) give useful structural information such as oxidation state of chemical species, site symmetry, and covalent bond strength.[24−27] In general, the small pre-edge peaks of the K-edge absorption spectra for transition metal compounds have been assigned to the transition from 1s to *n*d orbitals, even though it is a dipole-forbidden transition. Since the transition is very sensitive to chemical environments, the pre-edge feature in XANES studies has been used to infer the local structure around the central atom. Some molecular orbital calculation studies have been reported that the pre-edge peak intensity is related to 3d and 4p orbital mixing by perturbation of site symmetry and increases gradually with the departure from a centrosymmetric environment.[28−30] On the other hand, extended X-ray absorption fine structure (EXAFS) spectra have provided many quantitative structural characterizations such as interatomic distance, coordination number, and Debye−Waller factor.[31−35] Since the EXAFS

* To whom all correspondence should be sent. E-mail: chulhyun@alchemy.yonsei.ac.kr. Fax: 82-02-361-7050.

10.1021/jp990753b CCC: $18.00
Published on Web 07/21/1999

refinement does not depend on the long-range order of atomic arrangement and is very sensitive to atomic local sites, it is a powerful technique for local structural analysis of partially substituted inorganic compounds.

In the present study, the local structures for chemically and electrochemically Li ion extracted $Li_yCo_{0.85}Al_{0.15}O_2$ compounds will be investigated on the basis of XAS study. In the case of Li ion extraction, the addition of 0.15 mol of Al atom into the lattice results in the sharper X-ray diffraction peaks rather than those of $LiCoO_2$. This fact shows that the long-range order has been maintained effectively even in acid solution since the Al elements support the layer structural framework for the extraction. With the confidence of structural stability in acid solution, therefore, the local structural variations of $Li_yCo_{0.85}Al_{0.15}O_2$ compounds will be investigated intensively with respect to the Li ion extraction.

Experimental Section

Synthesis. Pristine $LiCo_{0.85}Al_{0.15}O_2$ compound has been prepared by the ceramic method from starting materials such as spectroscopic pure Li_2CO_3, Co_3O_4, and Al_2O_3 powders. The appropriate mixture has been prefired at 500 °C for 6 h under air atmosphere. The powder has been sintered at 780 °C for 48 h and then cooled to room temperature with slow cooling rate of about 1 °C/min. The grinding and heat treatment have been repeated in order to prepare the homogeneous solid solution. The homogeneous uniphase of the pristine compound has been identified with X-ray diffraction (XRD) analysis. The X-ray diffraction pattern was obtained with the Phillips X-ray diffractometer with Ni-filtered Cu K_α radiation by using Si powder as a standard. The bulk structure of the pristine compound has been characterized with Rietveld refinement, where the structural parameters such as lattice parameter, atomic coordinate, and occupancy could be determined accurately.

Chemically Li ion extraction from the pristine $LiCo_{0.85}Al_{0.15}O_2$ has been carried out in 1.4 M H_2SO_4 solution at room temperature. The pristine compound has been stirred in the acid solution for 1, 3, 6, 12, and 24 h, respectively. The obtained powders have been thoroughly washed with distilled water and then dried in vacuum. From their XRD patterns, it is found that the bulk structures have not been broken with the acid solution treatment. The mole fraction of the Co^{IV} ion to total Co ion could be determined quantitatively by the potentiometric titration in which I_2 formed by reduction of both Co^{III} and Co^{IV} ions to Co^{II} ion in KI solution is titrated with standard sodium thiosulfate solution in nitrogen atmosphere.

On the other hand, the Li ion has been electrochemically extracted in Li/EC, DEC, $LiPF_6$ (1:1:1 M)/$LiCo_{0.85}Al_{0.15}O_2$ cell with current density of 800 μA/cm^2 in voltage region between 3.0 and 4.3 V. After the first Li ion extraction (1 cycle), the successive Li ion insertion/extraction processes have been repeated three and five times (3 and 5 cycles).

Co K-Edge XAS Measurement. Co K-edge X-ray absorption spectra (XAS) have been recorded on the BL3C1 beam line of Pohang Light Source (PLS) with the ring current of 120−150 mA at 2.0 GeV. A Si(111) monochromator crystal has been used with detuning to 70% in intensity to eliminate the high-order harmonics. The data have been collected in transmission mode, with the nitrogen (85%) and argon (15%) gas-filled ionization chambers as detectors. Energy calibrations have been carried out with the Co metal foil assigning the first inflection point to 7709 eV. To remove an energy shift problem, the X-ray absorption spectrum for Co metal foil has been measured simultaneously in every measurements as the metal foil was positioned in front of the window of the third ion chamber. To investigate accurately the XANES spectra for the electronic transition to bound states, the data have been taken with step size of 0.2 eV in the XANES region.

Co K-Edge EXAFS Data Analysis. The normalized k^3-weighted EXAFS spectra, $k^3\chi(k)$, could be obtained when background removal and normalization processes have been carried out on the edge jump of ~7721 eV. The $k^3\chi(k)$ spectra have been Fourier transformed in the k range from 2.8 to 14.0 Å^{-1} to show the contribution of each bond pair on the Fourier transform (FT) peak. The experimental Fourier-filtered $k^3\chi(k)$ spectra could be obtained from the inverse Fourier transformation with the hanning window function in the r space range between 1.0 and 6.0 Å. To determine the structural parameters for each bond pair, the curve-fitting process has been carried out by using the EXAFS formula, which can be expressed as follows:

$$\chi(k) = \frac{\mu(E) - \mu_o(E)}{\mu_o(E)} = \sum N_j S_i^2(k) F_j(k) \exp(-2\sigma_j^2 k^2) \exp(-2r_j/\lambda_j(k)) \frac{\sin(2kr_j + \Phi_{ij}(k))}{kr_j^2}$$

which includes the photoelectron wave vector, k ($=[8\pi^2 m(E - E_o)/h^2]^{1/2}$), the coordination number, N_j, the amplitude reduction factor, S_i^2, the effective curved wave backscattering amplitude, $F_j(k)$, the Debye−Waller factor, σ_j^2, the mean free path of the photoelectron, λ, the interatomic distance, r_j, and total phase shift, Φ_{ij}, respectively.

Theoretical scattering paths could be obtained from the crystallographic description of the known $LiCoO_2$ model. The theoretical EXAFS parameters such as phase shift, backscattering amplitude, and total central atom loss factor have been calculated for a function of wavenumber for all possible scattering paths by FEFF6.01 code.[27,29] For simplicity in the curve fitting process, the S_i^2 value has been fixed to 0.85 for the Co atom. The coordination numbers (N) have been also fixed to the crystallographic values, since the N value is highly correlated with the Debye−Waller factor in the amplitude of EXAFS spectra. The experimental $k^3\chi(k)$ spectra could be fitted with possible scattering paths showing the substantial amplitude for the corresponding FT peak. In that case, only two structural parameters of the interatomic distance and the Debye−Waller factor could be used as adjustable parameters on the fitting process for the EXAFS spectra.

Results and Discussion

XRD and Chemical Analysis. Figure 1 shows XRD patterns with respect to extraction times for chemically Li ion extracted $Li_yCo_{0.85}Al_{0.15}O_2$ compounds. To specify the atomic distributions in the pristine $LiCo_{0.85}Al_{0.15}O_2$, the Rietveld refinement for the XRD pattern has been carried out by using hexagonal axes of $R\bar{3}m$ site symmetry. The Li atom is positioned at 3b (0, 0, 0.5), the Co/Al atom at 3a (0, 0, 0), and the O atom at 6c (0, 0, 0.24), respectively. The oxygen octahedra of the central Co/Al atom are shared each other with an octahedral edge within the *ab* plane and the Li atoms are placed in the lattice channel between the *ab* planes. The XRD patterns for chemical extraction show that the layer structures with two-dimensional framework have not been broken, even by acid treatment in 1.4 M H_2SO_4 solution.

As listed in Table 1, the *c*/*a* value for the Li ion extraction increases relative to that of the pristine compound, which means

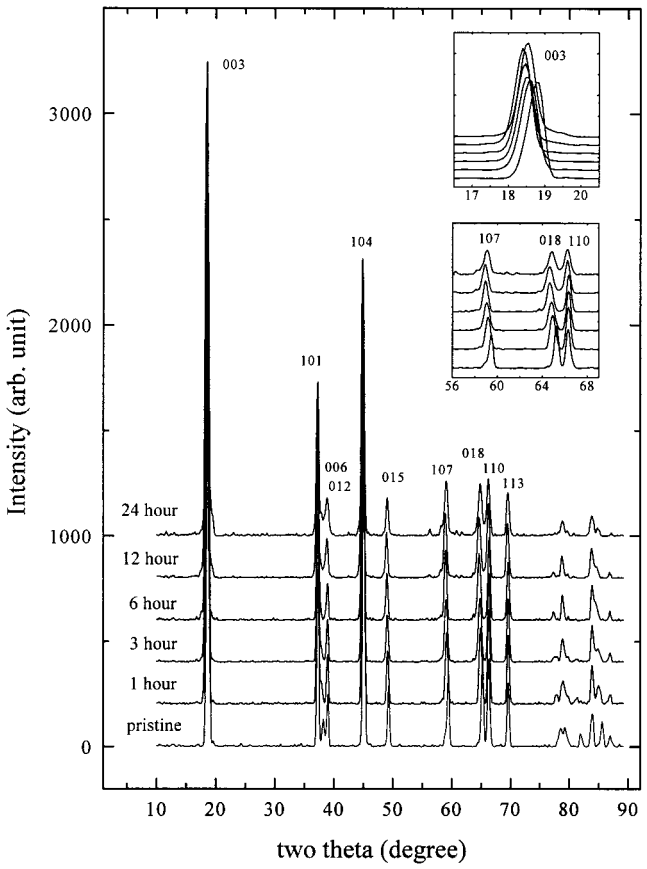

Figure 1. XRD patterns with respect to extraction time of chemically Li ion extracted $Li_yCo_{0.85}Al_{0.15}O_2$ compounds.

TABLE 1: Lattice Parameters and the Average Oxidation States of Co Ion for the Extraction Time of Chemically Li Ion Extracted $Li_yCo_{0.85}Al_{0.15}O_2$ Compounds

extraction time (h)	lattice parameter (Å)		lattice volume (Å^3)	c/a	average oxidation state of Co ion[a]
	a (Å)	c (Å)			
pristine	2.8178	14.0943	96.916	5.00	3.00
1	2.8136	14.1847	97.247	5.04	3.25
3	2.8124	14.2308	97.460	5.06	3.39
6	2.8118	14.2494	97.566	5.07	3.48
12	2.8128	14.2368	97.549	5.06	3.54
24	2.8134	14.2087	97.398	5.05	3.51

[a] The values have been obtained from the chemical analysis with the accuracy of ±0.02.

that the Li ion extraction leads to the shrinkage of interatomic distance within the *ab* plane and the increase of interplanar distance between *ab* planes. The increase of interplanar distance is due to the electrostatic repulsion between *ab* planes by the removal of Li ion. The chemical extraction after 6 h has little effect on the bulk structure, although the c/a value decreases slightly. In the case, the local structural variation around the Co atom by the Li ion extraction could not be critically discussed with the XRD patterns. Only the systematic variation of bulk structure could be determined since the structural characterization with XRD has been limited to average bulk structural property by long-range ordering. The more detailed local structure around the Co atom will be studied intensively with Co K-edge X-ray absorption spectroscopy.

From chemical analysis, it is found that only Co^{III} ion is located within the layer structure of the pristine $LiCo_{0.85}Al_{0.15}O_2$. After the chemical extraction for 1 h in 1.4 M H_2SO_4 solution, the average oxidation state of Co ion is changed from 3.00 to about 3.25, where the mole ratio of Co^{III} to Co^{IV} ions corresponds to about 3:1. The successive oxidation reaction has continued during the acid treatment of 12 h. The average oxidation state of Co ion increases up to 3.54. Thus, the average oxidation state of Co ion increases systematically with extraction time in 1.4 M H_2SO_4 solution.

However, the additional acid treatment after 12 h has little effect on the oxidation state of Co ion. The more chemical Li ion extraction has not been allowed by the structural destabilization in the view of the bulk property. On the contrary, the acid treatment for 24 h results in the small decrease of average oxidation state of Co ion. The fact shows that the saturated Co^{IV} ion has been partially reduced to Co^{III} ion. To maintain the bulk structural stabilization in the higher extracted condition, the H^+ ion in the acid solution may be simultaneously inserted into the empty Li^+ ion site.

Co K-Edge XANES Spectroscopy. Co K-edge XANES spectra and their pre-edge features of chemically and electrochemically Li ion extracted $Li_yCo_{0.85}Al_{0.15}O_2$ are shown in parts a and b of Figure 2, respectively. All XANES spectra have been normalized in order to compare their relative absorption peak feature quantitatively independent of structural variation. To show the peak features clearly, the second derivatives of XANES spectra have been obtained after the subtraction of the arctangent curve corresponding to the transition of the core electron to continuum states. For the chemical extraction, the second derivative peaks have been shown in Figure 3 and described with a Lorentzian function profile in Table 2 in order to determine the accurate peak positions and intensities.

For the pristine $LiCo_{0.85}Al_{0.15}O_2$, a weak absorption A peak at ~7709.9 eV represents the transition of the 1s electron to an unoccupied 3d−e_g orbital of Co^{III} ion with a low-spin (t_{2g}^6, $^1A_{1g}$) electronic configuration. Although the 1s → 3d transition is an electric dipole-forbidden transition in an ideal octahedral symmetry, the appearance of a weak absorption peak is due to pure electric quadrupole coupling and the noncentrosymmetric environment of slightly distorted CoO_6 octahedral site. Both B and C peaks appear due to the electric dipole-allowed transition of a 1s core electron to an unoccupied 4p bound state with T_{1u} symmetry. The B and C peaks correspond to two final states of a $1s^1c3d^7\underline{L}4p^1$ with shakedown process by ligand to metal charge transfer ($\underline{L}$MCT) and a $1s^1c3d^64p^1$ without shakedown process, respectively, where c and $\underline{L}$ are a 1s core hole and a ligand hole. The strong B peak occurs as a shoulder on the lower energy region of ~8.6 eV with respect to main absorption C peak at ~7727.8 eV since the 1s core electron of $3d^7\underline{L}$ state is less bounded on the more screened nucleus with respect to that of $3d^6$ state.

In the present XANES spectrum of the pristine compound, the strong appearance of LMCT process gives important information about the ground state of Co atom, which shows there are two kinds of bound states, $3d^7\underline{L}$ and $3d^6$ states. The fact can be supported by previous studies of configuration−interaction (CI) calculations and ^{57}Co solid-state NMR spectra for $LiCoO_2$ compound.[36,37] In the cluster CI calculation, the ground state of Co atom has been described with a substantial β value in $\alpha|3d^6\rangle + \beta|3d^7\underline{L}\rangle$, where the relative β value represents the degree of covalent character by Co 3d−O 2p hybridization. Also, the existence of at least two Co atomic sites in $LiCoO_2$, a diamagnetic low-spin Co^{III} ($t_{2g}^6e_g^0$) and a paramagnetic low-spin Co^{II} ($t_{2g}^6e_g^1$), has been presented from ^{57}Co NMR and ESR spectra. Both the large β value and the existence of paramagnetic Co^{II} ion show that the $|3d^7\underline{L}\rangle$ state by the LMCT process cannot be negligible as the ground state. From the appearance of a strong B peak for the present $LiCo_{0.85}Al_{0.15}O_2$,

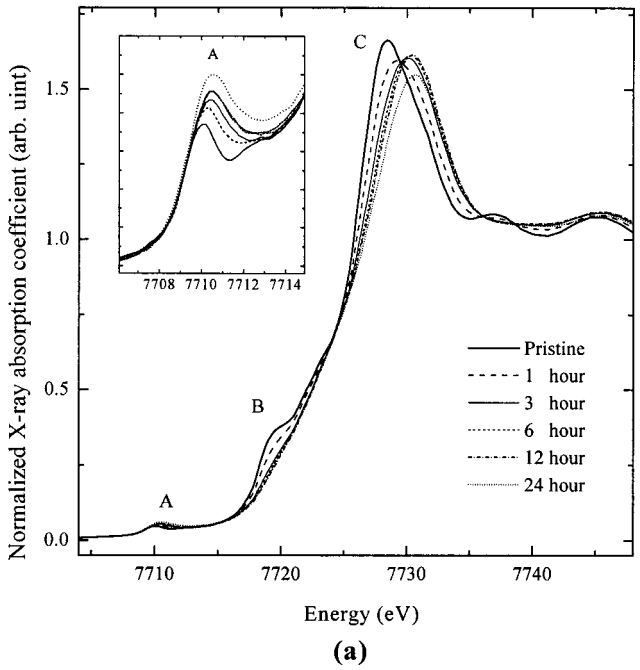

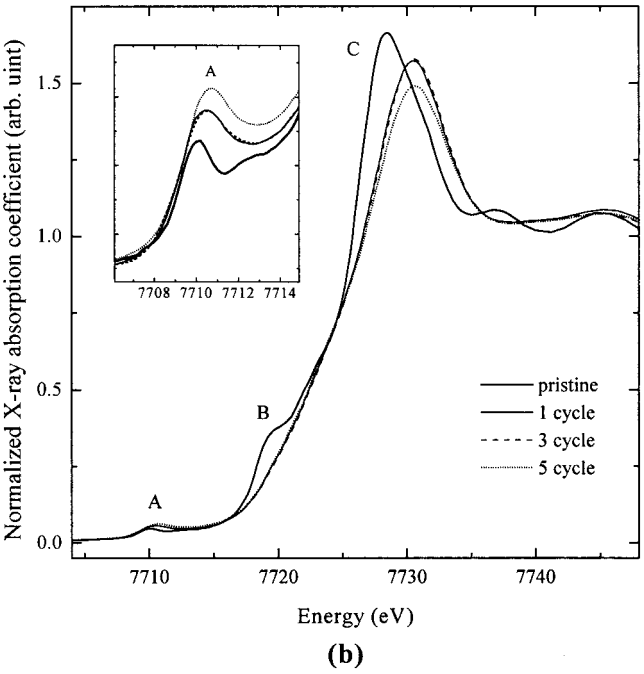

Figure 2. Normalized Co K-edge XANES spectra for (a) chemically and (b) electrochemically Li ion extracted $Li_yCo_{0.85}Al_{0.15}O_2$ compounds. The inset shows the pre-edge feature with the normalized absorption scale from 0.0 to 0.08.

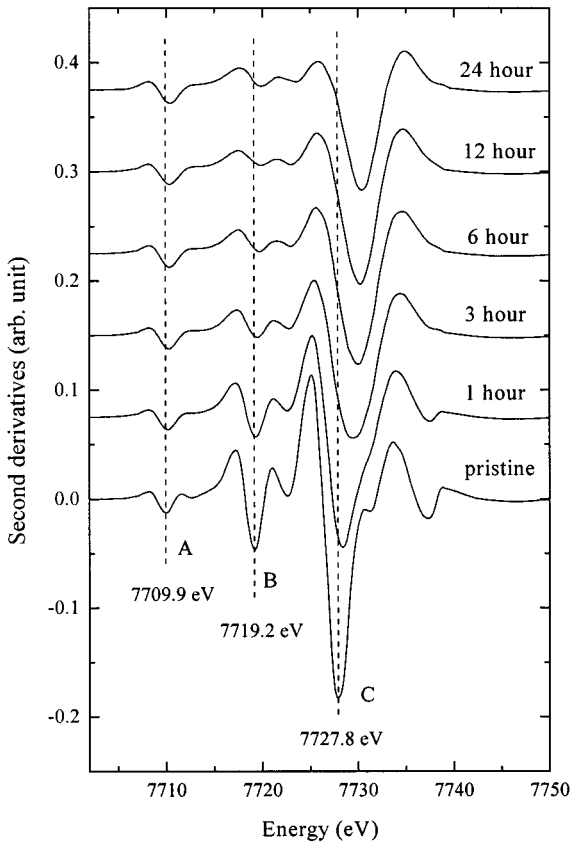

Figure 3. The second derivative curves of the normalized Co K-edge XANES spectra for chemically Li ion extracted $Li_yCo_{0.85}Al_{0.15}O_2$ compounds.

TABLE 2: Peak Position (*E*) and Intensity (*I*) for Co K-edge XANES Spectra with the Extraction Time in the Chemically Li Ion Extracted $Li_yCo_{0.85}Al_{0.15}O_2$ Compounds[a]

extraction time (h)	A peak		B peak		C peak	
	E (eV)	I_A	*E* (eV)	I_B	*E* (eV)	I_C
pristine	7709.9	0.029	7719.2	0.16	7727.8	1.01
1	7710.2	0.041	7719.2	0.08	7728.6	0.88
3	7710.3	0.047	7719.4	0.03	7729.4	0.75
6	7710.6	0.049	7719.5	0.03	7729.9	0.71
12	7710.6	0.049	7719.7	0.02	7730.2	0.68
24	7710.5	0.052	7719.7	0.02	7730.3	0.64

[a] Each peaks has been fitted with the Lorentzian function, $f(E) = 2A\Gamma/\pi\{\Gamma^2 + 4(E - E_c)^2\}$, where *E*, *A*, and Γ represent peak position, peak area, and full width at half-maximum (fwhm) of the peak, respectively.

therefore, it is sure that the ground state of the Co atom can be described as an equilibrium of $Co^{III}(t_{2g}^6e_g^0) + O^{2-}(2p^6) \leftrightarrow Co^{II}(t_{2g}^6e_g^1) + O^-(2p^5)$. From the intensity ratio of the B and C peaks, it can be estimated that the equilibrium is relatively shifted toward the $|3d^6\rangle$ state rather than the $|3d^7\underline{L}\rangle$ state.

As shown in Figure 2a, the XANES spectra for chemical extraction have been changed effectively with extraction time in 1.4 M H_2SO_4 solution. As the extraction time increases, the A peak broadens toward the higher energy region and its total peak intensity increases, while both B and C peaks are also shifted to higher energy, but their intensity decreases systematically. Since the peak features are very sensitive to the oxidation state of the central Co atom, the bond covalenecy, and the local structure around the Co atom, the structural variation for the Li ion extraction can be discussed with peak position and peak intensity in the present XANES spectroscopic study.

Figure 4 illustrates the relationship between the peak features (position and intensity) and the average oxidation state of Co ion. In these cases, the average oxidation state of Co ion for each extraction time has been introduced from the chemical analysis. At first, the linear relationship represents that the peak position is proportional to the average oxidation state of Co ion within the $Li_yCo_{0.85}Al_{0.15}O_2$. The A peak shift toward the higher energy region shows directly the partial evolution of Co^{IV} ion with the chemical extraction. It is reasonable that the higher absorption energy is necessary for the Co^{IV} environment in order to excite the 1s core electron which is strongly bounded to the less screened nucleus. From the A peak feature for the Li ion extraction, therefore, the broad A peak can be described to be composed of two 1s → 3d quadrupole transitions for Co^{III} and

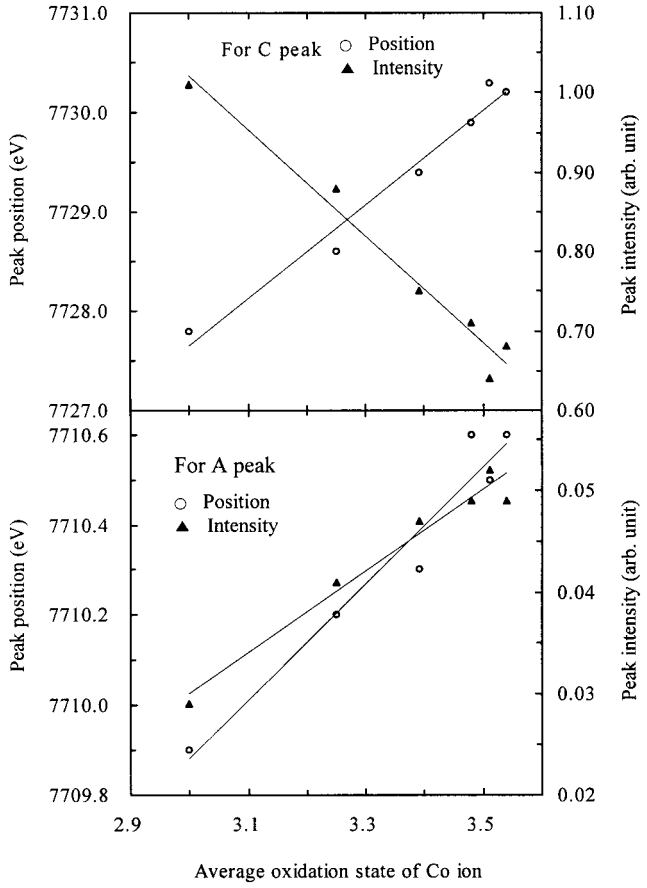

Figure 4. Relationship between the peak feature ((○) position and (▲) intensity) and the average oxidation state of Co ion (the lower part for A peak and the upper part for C peak).

Co^{IV} ions. The relative increase of peak intensity at the higher energy region of ~0.6 eV shows a gradual evolution of Co^{IV} ion with the chemical extraction. However, a quantitative composition ratio of two different oxidative ions could not be determined from the present A peak feature, since any remarkable separation between Co^{III} and Co^{IV} ions could not be shown with the energy resolution ($\Delta E/E$) of $\sim 2.0 \times 10^{-4}$ eV in the pre-edge region. Only systematic variation of the A peak position has been observed, showing the increase of the average oxidation state with the Li ion extraction.

The main absorption C peak feature also shows clearly the substantial difference in the oxidation state of Co ions with chemical extraction, as in the case of the A peak. The narrow and intense C peak of the pristine compound is changed to be broad toward the higher energy region after the chemical extraction. In particular, the C peak of the higher chemical extractions has been shifted toward the higher energy region of even ~2.5 eV with respect to that of the pristine. The fact represents that the chemical extraction leads to the existence of central atoms with the different chemical bonding characters of $Co^{III}-O$ and $Co^{IV}-O$ bonds where the $Co^{IV}-O$ bond is more covalent than the $Co^{III}-O$ bond. In the molecular orbital (MO) theory, the greater overlap between Co 4p and O 2p orbitals by the increased $Co^{IV}-O$ bond covalency results in an increase of the energy of the antibonding molecular level with T_{1u} symmetry. The higher absorption energy is necessary for $1s \rightarrow 4p$ dipole transition in the case of the $Co^{IV}-O$ bond. Therefore, the C peak feature for the higher extraction shows the increase of Co−O bond covalency in the CoO_6 octahedral layers. The fact is in good agreement with the result of an XRD study in which the atomic arrangements within the interplanar *ab* plane have shrunk for the Li ion extraction by the increase of crystallographic *c*/*a* value.

The variation of the peak intensity with the chemical extraction can give other structural information about the local structural environment around Co atom since it is very sensitive to the site symmetry and the density of empty bound state. As shown in the Figure 4, the A and C peak intensities show different dependence on the oxidation state. As mentioned above, the pre-edge peak intensity of $1s \rightarrow 3d$ electric quadrupole transition depends on the pure 3d character of the corresponding bound state under an ideal octahedral symmetry. In the noncentrosymmetric environment, however, the peak intensity is changed with the relative Co 3d−4p character mixing ratio since the local structural distortion on the Co atom gives rise to 3d−4p orbital mixing. On the orbital mixing, the $1s \rightarrow 3d$ quadrupole transition has obtained the electric dipole coupling by the partial possession of p character ($1s \rightarrow 3d + xp$ transition where the *x* value represents the degree of orbital mixing). Since the electric dipole coupling is generally much stronger than the electric quadrupole coupling by 2 orders magnitudes, even a small addition of 4p character into the 3d orbital has a significant effect on the pre-edge peak intensity. From the systematic increase of the A peak intensity, it is found out that the Li ion extraction leads to a local structural distortion around the Co atom, and the degree of structural distortion is proportional to the average oxidation state of Co ion.

The small decrease of p character by Co 3d−4p orbital mixing in the $1s \rightarrow 4p$ electric dipole transition leads to the systematic decrease of B and C peak intensities, corresponding to $1s \rightarrow 4p-xp$ transitions, with shakedown process and without shakedown process, respectively. In the viewpoint of bond covalency, however, the B peak intensity should have increased with the oxidation state of Co ion since the relatively small interatomic distance means a large β value of $|3d^7\underline{L}\rangle$ state, according to the reciprocal relationship between the transfer integral, T_{3d-2p}, and the interatomic distance ($T_{3d-2p} \approx \beta \approx 1/R^{3.5}$).[36] On the contrary, the B peak nearly disappears by the Li ion extraction with respect to the C peak. The incompatible B peak feature can be explained with the main contribution of local structural distortion by the formation of Co^{IV} ion. Since the mismatched Co 3d−O 2p orbital overlap by the tilted arrangement of the CoO_6 octahedra leads to the decrease of the transfer integral, it is difficult for the LMCT process to occur in the higher extractions, despite the small interatomic distance of Co−O bond.

On the basis of the relative changes of B and C peak intensities, therefore, the ground state of the Co atom can be discussed for the Li ion extraction. Figure 5 illustrates the dependence of peak intensity ratio (I_B/I_C) for the B and C peaks on the average oxidation state of Co ion. Since the relative I_B/I_C value corresponds to the degree of contribution of $|3d^7\underline{L}\rangle$ state to the ground state, the very small I_B/I_C value of the higher extraction shows the $|3d^7\underline{L}\rangle$ state can no longer be considered as a bound state. The significant decrease of the I_B/I_C value shows that the Li ion extraction gives rise to transition of the hole state ($\underline{L}$) from oxygen to Co atom. In the higher extractions, the $|3d^7\underline{L}\rangle$ state of the LMCT process is replaced by the $|3d^5\rangle$ state of the Co^{IV} ion as an another hole state, which means that the hole state is relatively localized at the Co atomic site under the local structural distorted environment. Therefore, the ground state of Co ion can be described as the mixed state between $|3d^6\rangle$ of Co^{III} and $|3d^5\rangle$ of Co^{IV}. Thus, the abrupt decrease of the B peak can be another proof of the local structural distortion

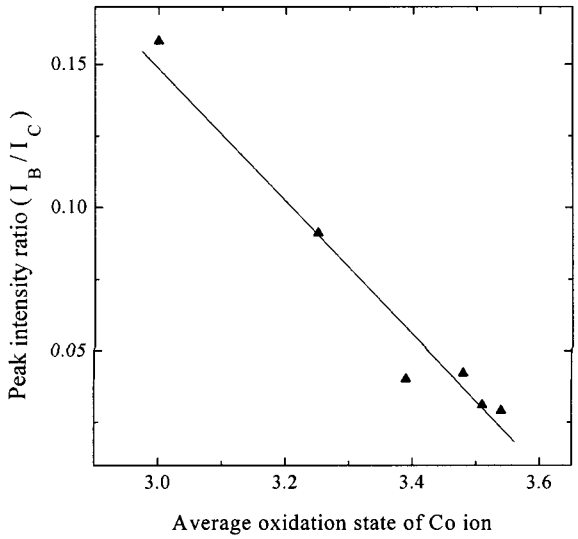

Figure 5. Dependence of peak intensity ratio (I_B/I_C) between B and C peaks on the average oxidation state of Co ion.

by the formation of the Co^{IV} ion, in addition to the increase in A peak intensity.

The electrochemical Li ion extraction also has strong effects on all peak features of Co K-edge XANES spectra, as shown in Figure 2b. Like in the case of the chemical extraction, the variations of peak features by the electrochemical extraction result from both the formation of Co^{IV} ion and local structural distortion. In the XANES features for two electrochemical extractions of the 1 and 3 cycles, there is no difference in the peak position and intensity, which represents that the electrochemical extraction/insertion processes are reversible until the 3 cycle. Namely, the oxidized Co^{IV} ions are completely reduced to Co^{III} ion when the extracted Li ion is inserted electrochemically into the interstitial channel of lattice. Until the 3 cycle of the electrochemical redox reaction, any variation of the local structure and the chemical composition could not be observed from the XANES spectra.

However, the XANES feature of the 5 cycle is different from those of the 1 and 3 cycles. There are significant variations of the peak position and intensity, which means the reversible redox reaction until the 3 cycle is changed to the irreversible reaction for the 5 cycle. If the redox reaction of the 5 cycle would be reversible, the XANES feature should have no change relative to those after the 1 and 3 cycles. The A and C peak shifts toward higher energy mean the relative increase of the mole fraction for Co^{IV} ion. Since all Co^{IV} ions after 3 cycle are not reduced completely to Co^{III} ion in the Li ion reinsertion process, the remaining Co^{IV} ion has contributed to the XANES feature of the 5 cycle, in addition to pure electrochemically oxidized Co^{IV} ions in the normally successive extraction process. In particular, both the increase of the A peak intensity and the decrease of the C peak intensity for the 5 cycle show that the large mole fraction of Co^{IV} ion leads to the higher Co 3d−4p orbital mixing by the structural distortion of CoO_6 octahedra.

Co K-Edge EXAFS Spectroscopy. The local structures around Co atom have been investigated with the normalized Co K-edge $k^3\chi(k)$ spectra for chemical and electrochemical Li ion extractions. Since the EXAFS spectral change for Li ion extraction is indicative of the local structural variation around Co atom, it is of interest to determine quantitatively the variation of each interatomic distance with the Li ion extraction.

Figure 6 shows the Fourier transforms (FT) of the $k^3\chi(k)$ spectra for the chemically and electrochemically Li ion extracted

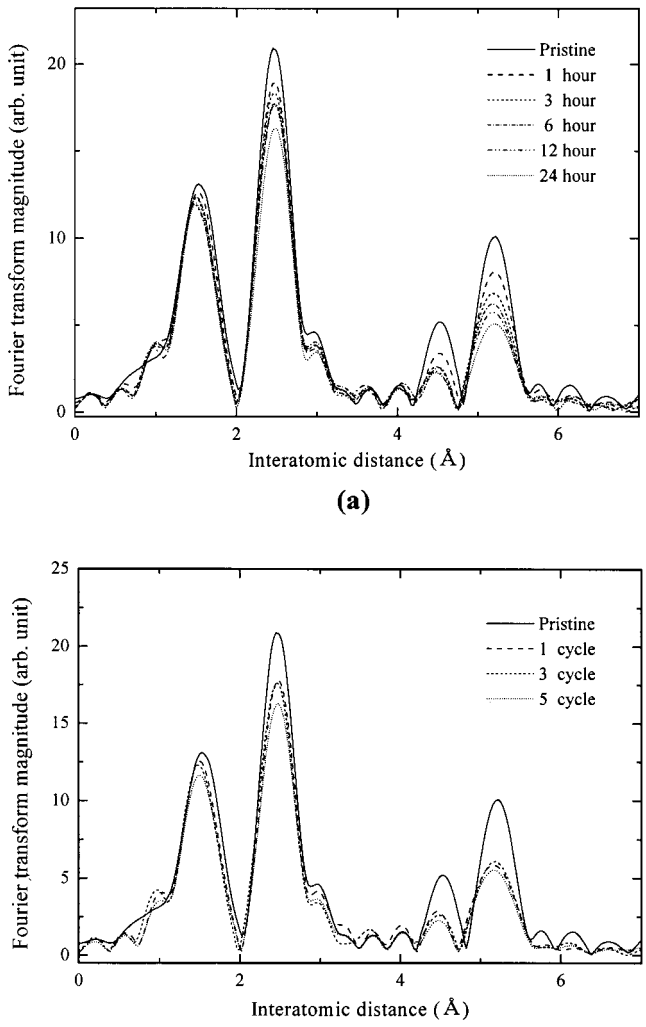

Figure 6. FT magnitudes of Co K-edge k^3-weighted EXAFS spectra as a function of interatomic distance for (a) the chemically and (b) the electrochemically Li ion extracted $Li_yCo_{0.85}Al_{0.15}O_2$ compounds.

$Li_yCo_{0.85}Al_{0.15}O_2$ compounds. The two large FT peaks between 1.0 and 3.5 Å are important to determine the correct structural information since the FT peaks are closely associated with the site symmetry around the central Co atom. The FT magnitude at ∼1.5 Å corresponds to six-coordinated oxygen of the nearest neighboring atom around the Co atom, while the other FT magnitude at ∼2.5 Å is assigned to the contribution by a six-coordinated Co/Al atom.

The higher FT peaks above ∼4.0 Å include practically a number of single and multiple scatterings. The separation of single and multiple scattering paths in the higher FT region is difficult because the scattering paths are highly overlapped with each other. The scattering paths may be negligible in the EXAFS refinements. As shown in Figure 6, however, the significant variation has been observed in the FT peaks above ∼4.0 Å, which means the more useful structural information for Li ion extraction can be provided with the FT peaks above ∼4.0 Å. Because of the importance for the FT peaks in the higher r region, the curve fitting process has been carried out until ∼6 Å. On the basis of the crystallographic description, Figure 7 shows the possible intraplanar scattering paths in the Co atomic array within the *ab* plane (except for oxygen atoms). For clarity, the contributions of Al atom to backscattering amplitude and phase shift function were not considered in the theoretical

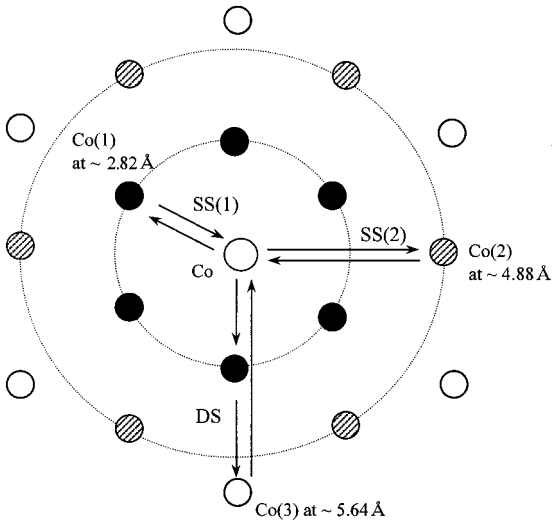

Figure 7. Possible intraplanar scattering paths in the Co atomic arrangements within the *ab* plane where SS(1), SS(2), and DS represent the single Co → Co(1), Co → Co(2), and the double Co → Co(1) → Co(3) scattering paths, respectively.

scattering calculation for the atomic array. In the region of $r \leq 6.0$ Å, the single and double scatterings are not the only types of scattering in the EXAFS spectroscopy. Usually, the higher multiple scattering paths may be significant rather than the single scattering in the higher r region. In the present EXAFS study, the multiple scattering with only 180° scattering angle has been considered by the focusing effect where the multiple scattering is enhanced as the scattering path approaches a linear arrangement. Some scatterings with an Li atom in an interstitial channel are neglected since the backscattering amplitude of the photoelectron with the Li ion is very weak.

As a result, the FT magnitude of ~4.5 Å is mainly contributed from two single scattering paths of intraplanar Co → Co/Al(2) and interplanar Co → Co/Al(I). The FT magnitude of ~5.3 Å includes four scattering paths which correspond to two single scattering paths of Co → Co/Al(3) and Co → Co/Al(II), a double scattering path of Co → Co/Al(1) → Co/Al(3), and a triple scattering path of Co → Co/Al(1) → Co/Al(3) → Co/Al(1). In these cases, the Co/Al(2) and Co/Al(3) atoms are located at the intraplanar *ab* plane, while the Co/Al(I) and Co/Al(II) atoms at the interplanar *ab* plane, respectively. All scattering paths are six degenerated, except for the double scattering Co → Co/Al(1) → Co/Al(3) path with 12-degeneracy.

Figure 8 shows the experimental Fourier-filtered (solid line) and best-fitted (dot) $k^3\chi(k)$ spectra and their Fourier transforms for the chemically Li ion extracted $Li_yCo_{0.85}Al_{0.15}O_2$ compounds. The structural parameters obtained from EXAFS refinement are listed in Table 3. For the pristine compound, the interatomic distance between Co and the nearest neighboring oxygen atom is estimated with 1.93 Å. In the second shell, the interatomic distance between Co and neighboring Co/Al atom is 2.82 Å. The values are in good agreement with those of XRD by Rietveld refinement. The interatomic distances of Co−O and Co−Co/Al(1) bonds for both chemical extractions of 6 and 12 h decrease to 1.91 and 2.79 Å, respectively. For the intraplanar scattering Co → Co/Al(2) and Co → Co/Al(1) → Co/Al(3) paths, with the major contribution on the corresponding FT magnitude of ~4.5 Å and ~5.3 Å, the interatomic distances were minimized by a decrease of ~0.04 Å in the higher Li ion extraction. The decreasing tendency of the interatomic distance is consistent with the XANES features, according to the general relationship between the peak position (E) and interatomic distance (R), $(E - E_o)R^2 =$ constant, where E_o is the threshold energy of 7709 eV in this case.[38] For the electrochemical extractions of the 1, 3, and 5 cycles, the interatomic distances for all bond pairs are similar to those for the chemical extractions of 6 and 12 h. Although the different XANES features between the 1 (or 3) and the 5 cycles were found out, any substantial

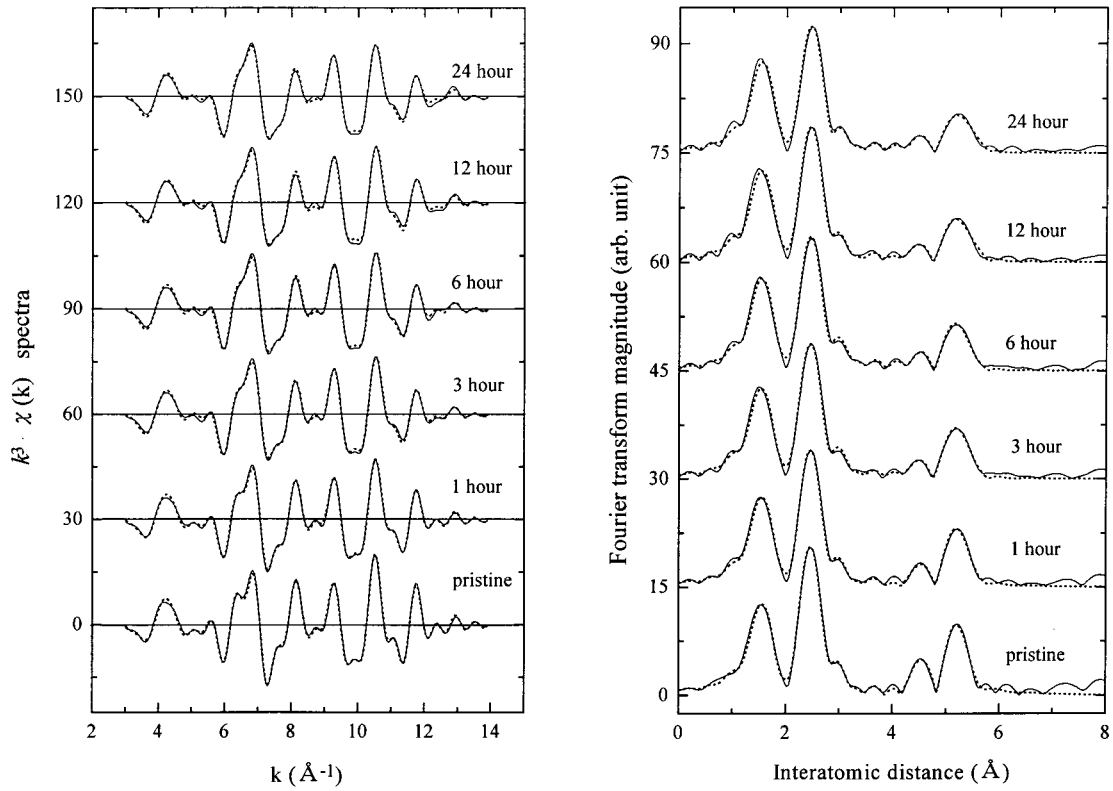

Figure 8. (a) Experimental Fourier-filtered (solid line) and the best-fitted (dot line) $k^3\chi(k)$ spectra and (b) Fourier transforms for chemically Li ion extracted $Li_yCo_{0.85}Al_{0.15}O_2$ compounds.

TABLE 3: Co K-Edge EXAFS Parameters for Chemically and Electrochemically Li Ion Extracted $Li_yCo_{0.85}Al_{0.15}O_2$ Compounds[a]

compound	path	N	ΔE (eV)	R (Å)[a]	σ^2 ($\times 10^{-3}$ Å^2)[a]
pristine	Co−O	6	−1.1	1.93	3.2
	Co−Co/Al(1)	6	−0.9	2.82	3.1
	Co−Co/Al(2)[b]	6	3.9	4.88	1.9
	Co−Co/Al(3)−Co/Al(1)[c]	12	−4.0	5.64	4.2
	For the Chemically Li Ion Extracted Compounds				
1 h	Co−O	6	0.9	1.92	3.6
	Co−Co/Al(1)	6	−1.2	2.81	3.7
	Co−Co/Al(2)	6	4.8	4.86	2.7
	Co−Co/Al(3)−Co/Al(1)	12	−4.2	5.61	5.0
3 h	Co−O	6	3.2	1.91	3.7
	Co−Co/Al(1)	6	−1.8	2.80	3.8
	Co−Co/Al(2)	6	6.0	4.84	3.4
	Co−Co/Al(3)−Co/Al(1)	12	−5.1	5.59	5.5
6 h	Co−O	6	3.6	1.91	3.7
	Co−Co/Al(1)	6	−1.7	2.79	3.9
	Co−Co/Al(2)	6	7.2	4.84	4.5
	Co−Co/Al(3)−Co/Al(1)	12	−5.0	5.59	5.9
12 h	Co−O	6	4.0	1.91	4.0
	Co−Co/Al(1)	6	−2.1	2.79	3.9
	Co−Co/Al(2)	6	5.8	4.84	4.8
	Co−Co/Al(3)−Co/Al(1)	12	−5.4	5.59	6.3
24 h	Co−O	6	4.2	1.91	4.0
	Co−Co/Al(1)	6	−2.1	2.80	4.2
	Co−Co/Al(2)	6	5.4	4.84	5.4
	Co−Co/Al(3)−Co/Al(1)	12	−4.6	5.59	6.7
	For the Electrochemicaly Li ion Extracted Compounds				
1 cycle	Co−O	6	3.7	1.91	4.3
	Co−Co/Al(1)	6	−2.9	2.79	3.8
	Co−Co/Al(2)	6	6.1	4.84	4.7
	Co−Co/Al(3)−Co/Al(1)	12	−6.5	5.59	6.3
3 cycle	Co−O	6	3.8	1.91	4.3
	Co−Co/Al(1)	6	−2.7	2.79	4.2
	Co−Co/Al(2)	6	5.7	4.84	5.2
	Co−Co/Al(3)−Co/Al(1)	12	−7.5	5.59	7.0
5 cycle	Co−O	6	3.2	1.91	4.6
	Co−Co/Al(1)	6	−3.0	2.79	4.4
	Co−Co/Al(2)	6	6.8	4.84	4.9
	Co−Co/Al(3)−Co/Al(1)	12	−8.2	5.58	6.9

[a] In all curve fitting process, the goodness of fit by $\{\sum(k^3\chi_{data} - k^3\chi_{model})^2\}/\sum(k^3\chi_{data})^2$ has been estimated within the allowed error range. The estimated errors are within ±0.02 Å for the interatomic distance and about 15% for the Debye−Waller factor. [b] The scattering paths have been selected from the largest contribution on the corresponding FT magnitude of ∼4.5 Å. [c] The scattering paths have been selected from the largest contribution on the corresponding FT magnitude of ∼5.3 Å.

difference between the interatomic distances after the electrochemical reversible and irreversible redox reactions could not be observed from EXAFS results.

In the FT peaks for the chemical and electrochemical extraction, the major variation has been observed in the magnitude of the FT peak rather than in the interatomic distance of each bond pair. The chemical and electrochemical Li ion extractions result in the substantial decrease of the FT magnitude for each bond pair. In particular, the FT magnitudes for chemical extraction have been changed systematically with extraction time. Moreover, the FT magnitude of ∼5.3 Å for the chemical extraction of the 24 h decreases significantly by a half magnitude.

The phenomena are reverse from the case of spinel $LiMn_2O_4$ compounds. In the previous studies for the spinel, the FT peaks of Mn−O and Mn−Mn bond pairs have increased with Li ion extraction from the interstitial channel of the spinel.[39,40] Since the Li ion extraction leads to a relative uniform oxidation state of Mn^{4+} from the mixed oxidation state of Mn^{3+} and Mn^{4+} ions, the increase of FT magnitude could be explained by the site ordered distribution, in addition to the decrease of the Jahn-Teller distorted Mn^{3+} sites in the octahedral symmetry.

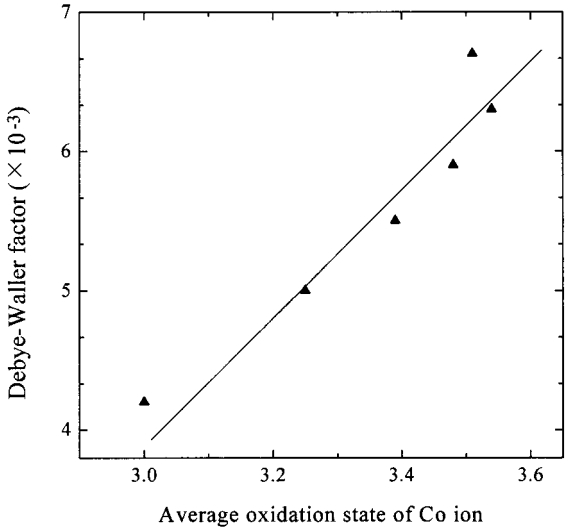

Figure 9. Linear relationship between the Debye−Waller factor of the focused Co → Co/Al(1) → Co/Al(3) double scattering and the average oxidation state of the Co ion.

Although the dependence of FT magnitude on the Li ion extraction in the present compound is different from that of the spinel, the FT variation results from the same origin in the viewpoint of the Debye−Waller factor. The magnitude of the FT peak is inversely related to the Debye−Waller factor that corresponds to the mean square relative displacement (MSRD) of interatomic distance for each bond pair due to static disorder and thermal vibrational disorder. In the present compounds, the systematic decrease of FT magnitudes results from the main contribution of static disorder to the MSRD rather than thermal vibrational effect. It is reasonable because the strong bond covalency by the increase of average oxidation state is indicative of the decrease of thermal vibrational disorder. Therefore, the decrease of FT magnitudes for the $Li_yCo_{0.85}Al_{0.15}O_2$ compounds is mainly associated with the static disorder of two different oxidative Co^{III} and Co^{IV} ions.

As listed in Table 3, the Li ion extraction gives rise to the increase of the Debye−Waller factor for all bond pairs. The Debye−Waller factor for the chemical extraction is proportional to the average oxidation state of the Co ion, which can be surely considered as a fingerprint for the static disorder of Co ions. For the Co−O bond pair, the small decrease of the FT magnitude is due to the disordered distribution of two kinds of the first shell, the Co^{III}−O and Co^{IV}−O bonds. In the case of the Co−Co/Al(1) bond, the different covalent bond pairs of Co^{III} (or Co^{IV})−Co^{III}/Al (or Co^{IV}/Al) lead to the systematic decrease of FT magnitude with the extraction time. In particular, it is of interest to discuss the FT peak at ∼5.3 Å showing the substantial dependence on the extraction time, where the focused double scattering of the Co → Co/Al(1) → Co/Al(3) path has the largest contribution to the FT magnitude. Figure 9 shows the linear relationship between the Debye−Waller factor of the focused double scattering and the average oxidation state. Since the double scattering path can experience more Co atomic sites, its Debye−Waller factor gives direct information about the disordering arrangement of Co ions. The Debye−Waller factor increases by ∼60% in the higher extractions relative to that of the pristine compound. Thus, the increase of the Debye−Waller factor with the Li ion extraction represents another proof for the formation of Co^{IV} ion in the $Li_yCo_{0.85}Al_{0.15}O_2$ compounds.

Conclusion

The chemical and electrochemical Li ion extractions from the two-dimensional framework of the $LiCo_{0.85}Al_{0.15}O_2$ compound have a large effect on the chemical and geometrical environments around the Co atom. From the peak position and intensity of the Co K-edge XANES spectra, it is concluded that the Li ion extraction leads to the increase in the average oxidation state of the Co ion and the local structural distortion around the Co atom. From the abrupt decrease of peak intensity for the 1s → 4p transition with shakedown process, it is found out that the ground states of the Co atom are transferred from a mixed state between $|3d^6\rangle$ and $|3d^7\underline{L}\rangle$ to a mixed state between $|3d^6\rangle$ and $|3d^5\rangle$, following the localization of hole state at the Co atomic site as a form of Co^{IV} ion by the structural distortion. For electrochemical extraction, the XANES features show that Li ion insertion/extraction processes are reversible for 3 cycles.

From the EXAFS study, the chemical and electrochemical extractions give rise to the decrease of interatomic distance for each bond pair. The systematic increase of the Debye−Waller factor has represented the static disorder of two kinds of different oxidative Co ions by the Li ion extraction. Thus, the Co K-edge EXAFS spectra give useful information about local structures around the Co atom that could not be determined in XRD study.

Acknowledgment. The present study was supported by Project 96-0501-0601-3 of the Korean Science and Engineering Foundation in 1997, and therefore, we express our appreciation to the authorities concerned. We are also grateful to Dr. Jae Min Lee and authorities of the Pohang Light Source (PLS) for X-ray absorption spectroscopic measurements.

References and Notes

(1) Hewston, T. A.; Chamberland, B. *J. Phys. Chem. Solids* **1987**, *48*, 97.
(2) Rossen, E.; Jones, C. W.; Dahn, J. R. *Solid State Ionics* **1992**, *57*, 311.
(3) Pickering, I. J.; George, G. W.; Lewandowski, J. T.; Jacobson, A. J. *J. Am. Chem. Soc.* **1993**, *115*, 4137.
(4) Kemp, J. P.; Cox, P. A. *J. Phys.: Condens. Matter.* **1990**, *2*, 9653.
(5) Reimers, J. N.; Dahn, J. R. *J. Electrochem. Soc.* **1992**, *139*, 2091.
(6) Broussely, M.; Perton, F.; Biensan, P.; Bodet, J. M.; Lecerf, A.; Delmas, C.; Rougier, A.; Peres, J. P. *J. Power Sources* **1995**, *54*, 54.
(7) Dahn, J. R.; Van Sacken, U.; Juzkow, M. W.; Al-Janaby, H. *J. Electrochem. Soc.* **1991**, *138*, 2207.
(8) Kumta, P. N.; Gallet, D.; Waghray, A.; Blomgren, G. E.; Setter, M. P. *J. Power Sources* **1998**, *72*, 91.
(9) Chiang, Y. M.; Jang, Y. I.; Wang, H. F.; Huang, B. Y.; Sadoway, D. R.; Ye, P. X. *J. Electrochem. Soc.* **1998**, *145*, 887.
(10) Ganguly, P.; Venkatraman, T. N.; Rajanohanan, P. R.; Ganapathy, S. *J. Phys. Chem. B* **1997**, *101*, 11099.
(11) Tukamoto, H.; West, A. R. *J. Electrochem. Soc.* **1997**, *144*, 3164.
(12) Jeong, E. D.; Won, M. S.; Shim, Y. B. *J. Power Sources* **1998**, *70*, 70.
(13) Numata, K.; Sakaki, C.; Yamanaka, S. *Chem. Lett.* **1997**, 725.
(14) Delmas, C.; Saadoune, I.; Rougier, A. *J. Power Sources* **1993**, *43*, 595.
(15) Ueda, A.; Ohzuku, T. *J. Electrochem. Soc*. **1994**, *141*, 2010.
(16) Alcantaro, R.; Morales, J.; Tirado, T. L.; Stoyanova, R.; Zhecheva, E. *J. Electrochem. Soc.* **1995**, *142*, 3997.
(17) Saadoune, I.; Delmas, C. *J. Mater. Chem.* **1996**, *6* (2), 193.
(18) Ceder, G.; Ching, Y. M.; Sadoway, D. R.; Aydinol, M. K.; Jang, Y. I.; Huang, B. *Science* **1998**, *392* (16), 694.
(19) Gupta, R.; Manthiram, A. *J. Solid State Chem.* **1996**, *121*, 483.
(20) Gummow, R. J.; Liles, D. C.; Thackeray, M. M. *Mater. Res. Bull.* **1993**, *28*, 1177.
(21) Dutta, G.; Manthiram, A.; Goodenough, J. B. *J. Solid State Chem.* **1992**, *96*, 123.
(22) Zhecheva, E.; Stoyanova, R. *J. Solid State Chem.* **1994**, *109*, 47.
(23) Stoyanova, R.; Zhecheva, E.; Zarkova, I. *Solid Sate Ionics* **1994**, *73*, 233.
(24) Shiro, Y.; Sato F.; Suzuki, T.; Iizuka, T.; Matsushita, T.; Oyanagi, H. *J. Am. Chem. Soc.* **1990**, *112*, 2921.
(25) Randall, C. R.; Shu, L.; Chiou, Y. M.; Hagen, K. S.; Ito, M.; Kitajima, N.; Lachicotte, R. J.; Zang, Y.; Que, L. *Inorg. Chem.* **1995**, *34*, 1036.
(26) Fronzoni, G.; Decleva, P.; Lisini, A. *Chem. Phys.* **1993**, *174*, 57.
(27) Rehr, J. J.; Leon, J. M.; Zabinsky, S. I.; Albers, R. C. *J. Am. Chem. Soc.* **1991**, *113*, 5135.
(28) Westre, T. E.; Kennepohl, P.; DeWitt, J. G.; Hedman, B.; Hodgson, K. O.; Solomon, E. I. *J. Am. Chem. Soc.* **1997**, *119*, 6297.
(29) O'Day, P. A.; Rehr, J. J.; Zabinsky, S. I.; Brown, G. E. *J. Am. Chem. Soc.* **1994**, *116*, 2938.
(30) Li, G. G.; Bridges, F.; Booth, C. H. *Phys. Rev. B* **1995**, *52*, 6332.
(31) Teo, B. K. *EXAFS: Basic Principles and Data Analysis*; Springer-Verlag: Berline, 1986.
(32) Koningsberger, D. C.; Prins, R. *X-ray Absorption: Principles, Applications, Techniques of EXAFS, SEXAFS and XANES*; Wiley-Interscience: New York, 1988.
(33) Ebbinghaus, S.; Fröba, M.; Reller, A. *J. Phys. Chem. B* **1997**, *101*, 9909.
(34) Zabinsky, S. I.; Rehr, J. J.; Ankudinov, A.; Albers, R. C.; Eller, M. J. *Phys. Rev. B* **1995**, *52*, 2995.
(35) Vaarkamp, M.; Dring, I.; Oldman, R. J.; Stern, E. A.; Koningsberger, D. C. *Phys. Rev. B* **1994**, *50*, 7872.
(36) Medarde, M.; Fontaine, A.; Garcia, J. L.; Rodriguez, J.; Santis, M.; Sacchi, M.; Rossi, G.; Lacorre, P. *Phys. Rev. B* **1992**, *46*, 14975.
(37) Gangury, P.; Venkatraman, T. N.; Rajamohanan, P. R.; Ganapathy, S. *J. Phys. Chem. B* **1997**, *101*, 11099.
(38) Natoli, C. R.; Benfatto, M.; Donaiach, S. *Phys. Rev. A* **1986**, *34*, 4682.
(39) Ammundsen, B.; Jones, D. J.; Roziere, J.; Burns, G. R. *Chem. Mater.* **1996**, *8*, 2799.
(40) Shiraishi, Y.; Nakai, I.; Tsubata, T.; Himeda, T.; Nishikawa, F. *J. Solid State Chem.* **1997**, *133*, 587.